IJIREEICE

ISSN (O) 2321-2004, ISSN (P) 2321-5526

International Journal of Innovative Research in Electrical, Electronics, Instrumentation and Control Engineering

Impact Factor 7.047 ⚟ Vol. 10, Issue 4, April 2022

DOI: 10.17148/IJIREEICE.2022.10457

# COMPREHENSIVE STUDY OF VARIOUS ALGORITHMS FOR DYNAMIC STATE ESTIMATION

**[1]Mr. Dixit Shah, [2]Dr. Dishang D. Trivedi[2]**

[1]P.G Scholar, Electrical Department, LDCE, Ahmedabad, Gujarat, India

[2] Associate Professor, Electrical Department, LDCE, Ahmedabad, Gujarat, India

**Abstract**: Precise power system dynamics estimation is essential for improving power system operation, analysis and control. Knowledge of power system dynamics is becoming more important as inverter-based energy sources get more integrated. Therefore, it is necessary to control a power system to evaluate the state variables of a network, but considering the economic confines simultaneous measurement of almost all electrical variables it's impossible. As a result, rather of measuring all of the states using sensors, it is preferable to estimate states. Extended kalman filter (EKF) and Unscented kalman filter (UKF) are used in this work to estimate the dynamic states of the power system (viz. rotor speed and rotor angle). Using WECC 3-machine 9-bus and IEEE 5-machine 14-bus test system, the approaches are validated. EKF and UKF are executed in MATLAB for comparative analysis. A load flow study is carried out initially on the WSCC 9-bus system, and a set of data from the load flow output is used as a measurement input in algorithms. Simulation results are show that the UKF and EKF can accurately estimate the power system dynamics

**Keywords**- Power system state estimation, extended kalman filter, and unscented kalman filter, ect.

## I. INTRODUCTION

Power system state estimation is an important tool of energy management system (EMS). Power system is observed by supervisory control system. These supervisory control systems also keep track of real-time system data. The goal of information collection is to ensure the safety of power system control and operation. However, due to measurement inaccuracies, communication noise, telemetry failures, and other factors, the information provided by the Supervisory Control and Data Acquisition (SCADA) system may not always be accurate. Although required quantities are not always readily available by measuring unit, power system control and operation requires information from the complete system. effective control and operation of power systems needs information from entire system. Power system state estimate deal with raw measurements and available data sets to find an approximated value of the required states.

Power system is dynamic in nature, because it changes very slowly with time and continuously. If the load on the system varies, the generations must adjust as well to overcome changes. Change in generation result the change in power flows and injections at the buses, thus nature of the power system changes from static to dynamic. Furthermore, the power system is becoming more dynamic as renewable energy resources, loads, and micro-grids become increasing. Controlling and monitoring the power system is very important since it is becoming the most complex system due to the integration of many renewable energy resources.

Static State Estimation (SSE), Tracking State Estimation (TSE), and Dynamic State Estimation (DSE) are the three types of state estimation methodologies. These dynamic behaviors of the power system are difficult to overcome by the SSE. This led to the development of an algorithm called DSE.

In the case of SSE, we only consider one measurement set at a time and estimate the matching state. Even when the estimation accuracy is within acceptable levels, SSE cannot forecast the future states of the system. Where, TSE estimates begin with the most recent estimated state, allowing for rapid state estimation. However, in both SSE and TSE, state estimates are computed using a single set of data and a single estimation step. DSE complete the estimation in two-step, so that DSE approach has a various advantages. The expected states are calculated in the first stage, which is known as the prediction step. The actual states of the system are computed in the next phase, which is known as the Correction step, using the calculated predicted states and the acquired measurement results. Because of the extra step in the DSE power system, the operator has more time to make control decisions in an emergency. For the estimating process, DSE considers both the measurement set and the projected state variables. The basic problem with DSE is that any quick changes in load

  

DOI: 10.17148/IJIREEICE.2022.10457

or generation produce a significant transition in the state variables. The state variables of the generator, such as rotor angle and speed, are affected by changes in active and reactive power.

The majority of monitoring and control systems used in control centers are based on static state estimates, which may not good enough to capturing such a changes. As a result, a highly accurate estimator that can track dynamic changes in nonlinear power systems on a continuous basis is required. The most often used Kalman filter algorithms for DSE are the Extended Kalman Filter (EKF) and Unscented Kalman Filter (UKF). Because power system equations (such as the swing equation and the power flow equation) are nonlinear, Kalman filters were used on the WSCC-9 and IEEE-14 buses. The rotor speed and angle of a generator were calculated using EKF and UKF in this study.

## II. EKF & UKF ALGORITHMS

**Dynamic State Estimation Algorithms**

The dynamic state estimation (DSE) algorithms determine by the system's dynamic states, which are state variables in the nonlinear algebraic equations that define the power system. The identification of mathematical modelling for the reliability of the power system is the first stage in the DSE process. DSE forecasts the dynamic state vector one step ahead of time using the system's mathematical model and the acquired measurement data. A set of nonlinear differential equations can be used to model a dynamic system.

$$\frac{dx}{dt} = f(x, u, w); \qquad \frac{2H}{\omega_s}\frac{d\omega}{dt} = T_M - P_e - D(\omega - \omega_s) + v$$

The state variables are represented by the x vector, the algebraic variables are represented by the u vector, and process (system) noise is represented by the w vector. The difference form of Eq.

$$\begin{aligned} x_k &= x_{k-1} + f(x_{k-1}, u_{k-1}, w_{k-1})\Delta t \\ &= g(x_{k-1}, u_{k-1}, w_{k-1}) \end{aligned}$$

Where, $k-1$ is the present instant of time index, $k$ is the next instant of time index and $\Delta t$ is the time step. The measurements at time step $k$ can be represented as a vector of non-linear functions $h(.)$. this is also called as measurement model of the power system dynamic state estimation.

$$z_k = h(x_k, v_k)$$

The resulting error between the measured and calculated values is given by

$$\epsilon_k = z_k - h(x_k, v_k)$$

As all dynamic variables (rotor speed and rotor angle) in power systems cannot be measured directly, they must be computed and estimated. This challenge can be solved by using Kalman Filter techniques in power system dynamic state estimation. The state variables in non-linear differential equations can be estimated using the EKF and UKF techniques. In the next sections, the EKF and UKF algorithms are presented.

- **EKF Algorithm**

The EKF is a nonlinear Kalman Filter that linearizes around a current mean and error covariance estimate.
The Extended kalman filter (UKF) can be summarized as follows:

1. The discrete time system equations of a non-linear system can be represented as

$$\begin{aligned} x_{k+1} &= f_k(x_k, u_k, w_k) \\ y_k &= h_k(x_k, v_k) \\ w_k &\sim (0, Q_k) \\ v_k &\sim (0, R_k) \end{aligned}$$

$Q_k$ indicates the system noise and $R_k$ indicates the measurement of noise covariance

2. The initial state covariance matrix is initialised by taking the second moment of the system state about the first estimate, and the initial state of EKF is initialised by taking the expectation of the initial state of the system.

It can be stated mathematically as follows.

$$\begin{aligned} \hat{x}_0^+ &= E(x_0) \\ P_0^+ &= E[(x_0 - \hat{x}_0^+)(x_0 - \hat{x}_0^+)^T] \end{aligned}$$

The state and error covariance matrix are predicted as follows for each time step k.

3. Partial derivative matrices of the current state estimate $\hat{x}_{k-1}^+$are obtained as follows.

$$F_k = \left.\frac{\partial f_k}{\partial x}\right|_{\hat{x}_{k-1}^+}$$

$$L_k = \left.\frac{\partial f_k}{\partial w}\right|_{\hat{x}_{k-1}^+}$$

International Journal of Innovative Research in Electrical, Electronics, Instrumentation and Control Engineering
Impact Factor 7.047 ⁘ Vol. 10, Issue 4, April 2022
DOI: 10.17148/IJIREEICE.2022.10457

4. The time update of state estimate and estimation-error covariance matrix is done using:

$$P_k^- = F_k P^+ k - 1 F_k^T + L_k Q_k L_k$$
$$\hat{x}_k^- = f_k(\hat{x}_{k-1}^+, u_{k-1}, 0)$$

The state and error covariance matrix correction is done as follows for each time step k.

5. Partial derivative matrices for correction are calculated as:

$$H_k = \left.\frac{\partial h_k}{\partial x}\right|_{\hat{x}_k^-}$$
$$V_k = \left.\frac{\partial h_k}{\partial v}\right|_{\hat{x}_k^-}$$

6. The state estimate and estimation error covariance are measured and updated as follows:

$$K_k = P_k^- H_k^T (H_k P_k^- H_k^T + V_k R_k V_k^T)^{-1}$$
$$\hat{x}_k^+ = \hat{x}_k^- + K_k[z_k - h_k(\hat{x}_k^-, 0)]$$
$$P_k^+ = (I - K_k H_k) P_k^-$$

- **UKF Algorithm**

The sigma-points computation, state prediction, and state correction are the three primary aspects of the UKF algorithm. The Unscented Kalman Filter (UKF) can be summarized as follows:

1. The discrete time system equations are presented as follows:

$$x_k = f_{k-1}(x_{k-1}, u_{k-1}, w_{k-1})$$
$$y_k = h_k(x_k, v_k)$$
$$w_k \sim (0, Q_k)$$
$$v_k \sim (0, R_k)$$

$Q_k$ indicates the system noise and $R_k$ indicates the measurement of noise covariance

2. Initialize the filter:

$$\hat{x}_0^+ = E(x_0)$$
$$P_0^+ = E[(x - \hat{x}_0^+)(x - \hat{x}_0^+)^T]$$

Where, $\hat{x}_0^+$ represents the initial state and $P_0^+$ represents the initial state covariance matrix. The subscript $+$ indicates the estimate is in an a posteriori estimate.

3. The state estimate and covariance are propagated from one measurement time to the next using the following time update equations.

(a) Firstly, to propagate from time step $k-1$ to $k$, the sigma points $\hat{x}_{k-1}^i$ are specified according to the following formula:

$$\hat{x}_{k-1}^{(i)} = \hat{x}_{k-1}^+ + \tilde{x}^{(i)},\ i = 1, \dots, 2n$$
$$\tilde{x}^{(i)} = \left(\sqrt{(n+\lambda)P_{k-1}^+}\right)_i^T,\ i = 1, \dots, n$$
$$\tilde{x}^{(n+i)} = -\left(\sqrt{(n+\lambda)P_{k-1}^+}\right)_i^T,\ i = 1, \dots, n$$

(b) Use the known nonlinear system equation $f(.)$ to transform the sigma points into $\hat{x}_k^{(i)}$ vectors as shown in Eq. with proper changes as our nonlinear transformation is $f(.)$ rather than $h(.)$ :

$$\hat{x}_{k-1}^{(i)} \xrightarrow{f(\cdot)} \hat{x}_k^{(i)},\ \hat{x}_k^{(i)} = f\left(\hat{x}_{k-1}^{(i)}, u_k, t_k\right)$$

(c) Combine the $\hat{x}_k^{(i)}$ vectors to obtain the a priori state estimate at time $k$ which is given by the following formula:

$$\hat{x}_k^- = \frac{1}{2n}\sum_{i=1}^{2n} \hat{x}_k^{(i)}$$

(d) Estimate the a priori error covariance by adding $Q_{k-1}$ to the end of the equation in order to take the process noise into account:

$$P_k^- = \frac{1}{2n}\sum_{i=1}^{2n} \left(\hat{x}_k^{(i)} - \hat{x}_k^-\right)\left(\hat{x}_k^{(i)} - \hat{x}_k^-\right)^T + Q_{k-1}$$

DOI: 10.17148/IJIREEICE.2022.10457

4. The time update equations are now complete, and the measurement update equations must be implemented in the UKF algorithm's final section.

(a) Choose sigma points $\hat{x}_k^{(i)}$ with proper changes since the current best assumption for the mean and covariance of $x_k$ are $\hat{x}_k^-$ and $P_k^-$:

$$\begin{aligned}\hat{x}_k^{(i)} &= \hat{x}_k^- + \tilde{x}^{(i)},\ i = 1, \dots, 2n \\ \tilde{x}^{(i)} &= \left(\sqrt{(n+\lambda)P_k^-}\right)_i^T,\ i = 1, \dots, n \\ \tilde{x}^{(n+i)} &= -\left(\sqrt{(n+\lambda)P_k^-}\right)_i^T,\ i = 1, \dots, n\end{aligned}$$

(b) Using the known nonlinear measurement equation $h(.)$ to transform the sigma points into $\hat{y}_k^{(i)}$ vectors as follow:

$$\hat{y}_k^{(i)} \xrightarrow{h(\cdot)} \hat{x}_k^{(i)},\ \hat{y}_k^{(i)} = h\left(\hat{x}_k^{(i)}, t_k\right)$$

(c) Combine the $\hat{y}_k^{(i)}$ vectors to obtain the predicted measurement at time:

$$\hat{y}_k = \frac{1}{2n}\sum_{i=1}^{2n} \hat{y}_k^{(i)}$$

(d) Add $R_k$ to the end of the equation to account for measurement noise and estimate the covariance of the projected measurement

$$P_y^- = \frac{1}{2n}\sum_{i=1}^{2n} \left(\hat{y}_k^{(i)} - \hat{y}_k\right)\left(\hat{y}_k^{(i)} - \hat{y}_k\right)^T + R_k$$

(e) Estimate the cross covariance between $\hat{x}_k^-$ and $\hat{y}_k$ :

$$P_{xy}^- = \frac{1}{2n}\sum_{i=1}^{2n} \left(\hat{x}_k^{(i)} - \hat{x}_k^-\right)\left(\hat{y}_k^{(i)} - \hat{y}_k\right)^T$$

(f) Finally, the normal Kalman filter formulae can be used to update the state estimate's measurement:

$$\begin{aligned}K_k &= P_{xy}P_y^{-1} \\ \hat{x}_k^+ &= \hat{x}_k^- + K_k(y_k - \hat{y}_k) \\ P_k^+ &= P_k^- - \left(K_k P_y K_k^T\right)\end{aligned}$$

Where, $K_k$ represents the Kalman gain matrix, $\hat{x}_k^+$ represents the state estimate and $P_k^+$ represents the estimation error covariance matrix.

## III. MATHEMATICAL FORMULATION

The data from the WSCC-9 and IEEE-14 buses is converted to a common base, which is typically 100 MVA. Electrical, mechanical and damping power are all expressed in per unit.

The Real and Reactive power of the load, $P_{Li}$ and $Q_{Li}$, will be obtained by executing load flow. If a load bus has a voltage solution $V_{Li}$ and complex power demand $S_{Li} = P_{Li} + jQ_{Li}$, then

$$y_{Li} = \frac{I_{Li}}{V_{Li}} = \frac{S_{Li}^*}{|V_{Li}|^2} = \frac{P_{Li} - jQ_{Li}}{|V_{Li}|^2}$$

The internal voltages of the generators $|E_i|\angle\delta_i{}^0$ are derived from the power flow data using the pre-disturbance terminal voltages $|V_{ai}|\angle\beta_i{}^0$.

$$|E_i|\angle\delta_i' = |V_{ai}| + jx_{di}I_i$$

$$\begin{aligned}|E_i|\angle\delta_i{}' &= |V_{ai}| + j\frac{x_{di}S_{Gi}^*}{|V_{ai}|} = |V_{ai}| + j\frac{x_{di}(P_{Gi} - jQ_{Gi})}{|V_{ai}|} \\ &= \left(|V_{ai}| + \frac{Q_{Gi}x_{di}}{|V_{ai}|}\right) + j\left(\frac{P_{Gi}x_{di}}{|V_{ai}|}\right)\end{aligned}$$

also

$$\delta_i^0 = \delta_i' + \beta_i.$$

Where, angle difference between internal and terminal voltage is $\delta_i'$.
Actual terminal voltage angle is $\beta_i$

Impact Factor 7.047 ⪤ Vol. 10, Issue 4, April 2022

DOI: 10.17148/IJIREEICE.2022.10457

Initial generator angle $\delta_i^0$

The $Y_{bus}$ matrices for the prefault, faulted and postfault network conditions are calculated. $Y_{bus}$ Further reduce by kron equation. (Here we assumed generated Emf as node)

$$I_n = (Y_{nn} - Y_{ns}Y_{ss}^{-1}Y_{sn})E_n = \hat{Y}E_n$$

Where, $\hat{Y}$ is the desired reduced admittance matrix; $Y_{nn}$ is diagonal matrix of inverted generator impedances; $Y_{ns}$ is created based on generator and bus connection,

$$Y_{nskm} = \begin{cases} \dfrac{-1}{jx_{dn}} & \text{if } m = G_n \text{ and } k = n \\ 0 & \text{otherwise.} \end{cases}$$

$Y_{ns}$ = transpose of $Y_{ns}$; $Y_{nn}$ = System bus admittance matrix (WSCC-9 BUS & IEEE-14) ;

Real power delivered to the network by i[th] machine is given as

$$P_{Gi} \quad = |E_i^2||\hat{Y}_{ii}|\cos(\theta_{ii}) + \sum_{\substack{j=1 \\ j\neq i}}^{n} |E_i||E_j||\hat{Y}_{ij}|\cos(\delta_i - \delta_j - \theta_{ij})$$

$$i = 1,2,\dots,n$$

To analyses the rotor behavior we can use swing equation. Generator rotor speeds and angles can be derived using swing equation,

$$M\frac{d\omega}{dt} = P_M - P_e - P_{di} \qquad\qquad \frac{d\delta}{dt} = \omega - \omega_s$$

Where, $P_e$ is measured or calculated using Real power eq[n]

$$M_i\frac{d\omega_i}{dt} = P_{mi} - E_i^2\hat{G}_{ii} - \sum_{\substack{j=1 \\ j\neq i}}^{n} |E_i||E_j|\begin{bmatrix} \hat{B}_{ij}\sin(\delta_i - \delta_j) \\ +\hat{G}_{ij}\cos(\delta_i - \delta_j) \end{bmatrix} - P_{di}$$

$$\frac{d\delta_i}{dt} = \omega_i,\ i = 1,2,\cdots,n.$$

Where, $\hat{G}_{ii} = |\hat{Y}_{ii}|\cos(\theta_{ii})$ is the short-circuit conductance;

$\hat{B}_{ij} = |\hat{Y}_{ij}|\sin(\theta_{ij})$ is the transfer susceptance;

$\hat{G}_{ij} = |\hat{Y}_{ij}|\cos(\theta_{ij})$ is the transfer conductance.

By implementing all this equation into EKF and UKF algorithm we can find estimated speed.

## IV. SIMULATION AND RESULTS

Extended kalman filter (EKF) and Unscented kalman filter (UKF) are used in this work to estimate the dynamic states of the power system (viz. rotor speed and rotor angle). Using WECC 3-machine 9-bus and IEEE 5-machine 14-bus test system, the approaches are validated. EKF and UKF are executed in MATLAB for comparative analysis. A load flow study is carried out initially on the WSCC 9-bus system, and a set of data from the load flow output is used as a measurement input in algorithms. Simulation results are show that the UKF and EKF can accurately estimate the power system dynamics.

**IJIREEICE** ISSN (O) 2321-2004, ISSN (P) 2321-5526

International Journal of Innovative Research in Electrical, Electronics, Instrumentation and Control Engineering

Impact Factor 7.047 ⋇ Vol. 10, Issue 4, April 2022

DOI: 10.17148/IJIREEICE.2022.10457

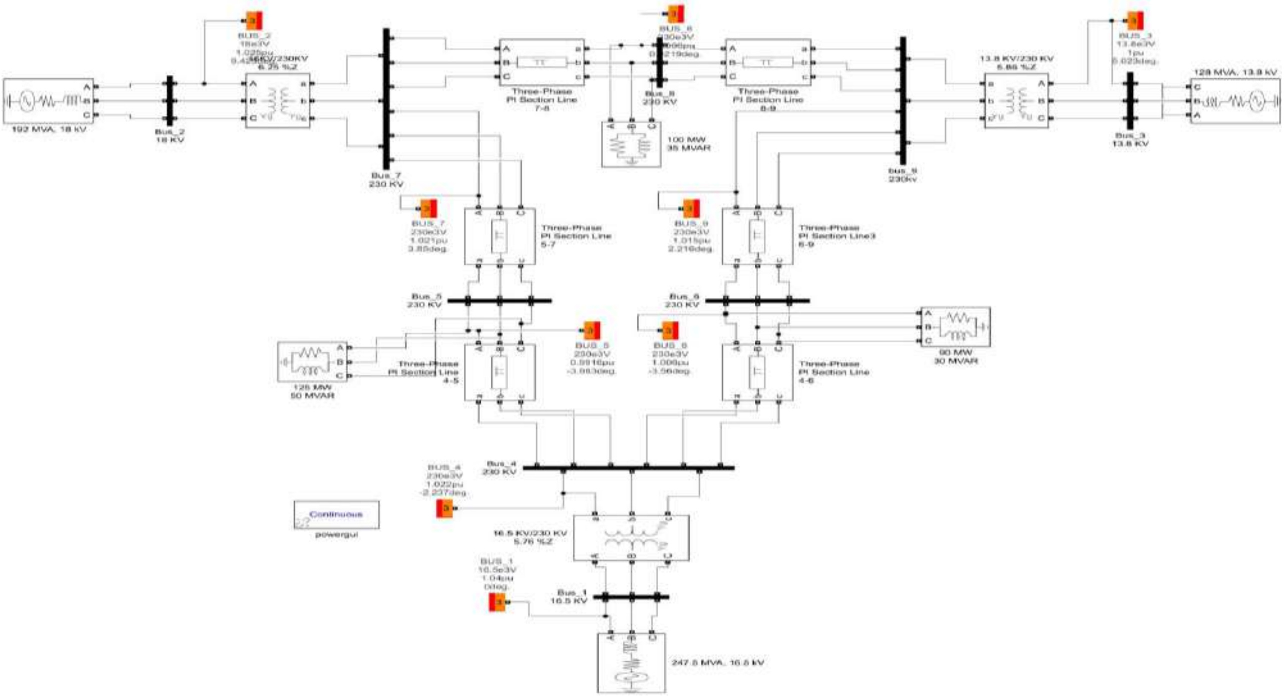


Fig 4.1- Loadflow of WSCC-9 bus system

Load Flow Analyzer

Model Units Help

Model: MATLAB_FSIM_WSCC9_BUS_3GE Update The load flow converged! The table shows the load flow solution. Click Apply to update the model with this solution. Compute Apply Add bus blocks Report

| Block name | Block type | Bus type | Bus ID | Vbase (kV) | Vref (pu) | Vangle (deg) | P (MW) | Q (Mvar) | Qmin (Mvar) | Qmax (Mvar) | V_LF (pu) | Vangle_LF (deg) | P_LF (MW) | Q_LF (MVA) |
|---|---|---|---|---|---|---|---|---|---|---|---|---|---|---|
| 192 MVA, 18 kV | Vsrc | PV | BUS_2 | 18.0000 | 1.0250 | 0 | 163.0000 | 0 | -99.0000 | 99.0000 | 1.0250 | 9.4287 | 163.0000 | 14.6655 |
| Load Flow Bus1 | Bus | - | BUS_7 | 230.0000 | 1.0000 | 0 | 0 | 0 | 0 | 0 | 1.0210 | 3.8496 | 0 | 0 |
| 100 MW 35 MVAR | RLC load | PQ | BUS_8 | 230.0000 | 1.0000 | 0 | 100.0000 | 35.0000 | -Inf | Inf | 1.0058 | 0.9219 | 100.0000 | 35.0000 |
| 125 MW 50 MVAR | RLC load | PQ | BUS_5 | 230.0000 | 1.0000 | 0 | 125.0000 | 50.0000 | -Inf | Inf | 0.9916 | -3.9829 | 125.0000 | 50.0000 |
| 128 MVA, 13.8 kV | Vsrc | PV | BUS_3 | 13.8000 | 1.0000 | 0 | 85.0000 | 0 | -99.0000 | 99.0000 | 1.0000 | 5.0228 | 85.0000 | -23.1889 |
| 90 MW 30 MVAR | RLC load | PQ | BUS_6 | 230.0000 | 1.0000 | 0 | 90.0000 | 30.0000 | -Inf | Inf | 1.0060 | -3.5604 | 90.0000 | 30.0000 |
| Load Flow Bus6 | Bus | - | BUS_9 | 230.0000 | 1.0250 | 0 | 0 | 0 | 0 | 0 | 1.0149 | 2.2163 | 0 | 0 |
| Load Flow Bus7 | Bus | - | BUS_4 | 230.0000 | 1.0000 | 0 | 0 | 0 | 0 | 0 | 1.0216 | -2.2369 | 0 | 0 |
| 247.5 MVA, 16.5 kV | Vsrc | swing | BUS_1 | 16.5000 | 1.0400 | 0 | 0 | 0 | -Inf | Inf | 1.0400 | 0 | 72.2149 | 34.8263 |

Fig 4.2- Loadflow Results of WSCC-9 bus system

**Simulation Results of WSCC-9 bus Using EKF & UKF**

We simulated WSCC-9 bus system when fault near bus 5 is occurs at 2s and stay in system for 0.12s. To remove the fault line 5-7 is removed at 2.12s. MATLAB results are presented in next table.

| Without Transient **: WOTR** \| With Transient **: WITR** | |
|---|---|
| 5.2.1 Simulation using **EKF** ( WOTR + WITR ) | 5.2.2 Simulation using **UKF** ( WOTR + WITR ) |
| 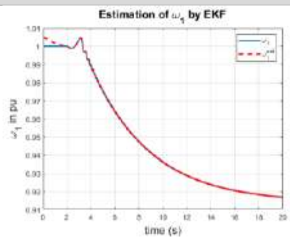  Fig 4.3- Rotor speed of Gen-1 WOTR using EKF | 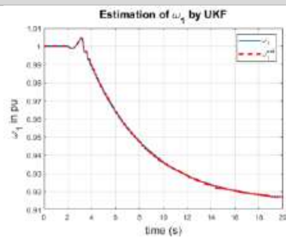  Fig 4.4- Rotor speed of Gen-1 WOTR using UKF |

International Journal of Innovative Research in Electrical, Electronics, Instrumentation and Control Engineering

Impact Factor 7.047 ⁙ Vol. 10, Issue 4, April 2022

DOI: 10.17148/IJIREEICE.2022.10457

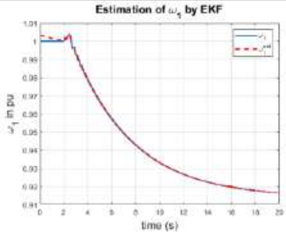


Fig 4.5- Rotor speed of Gen-1 WITR using EKF

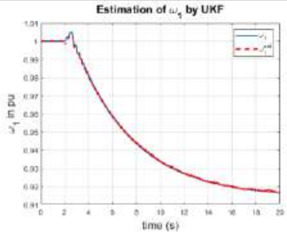


Fig 4.6- Rotor speed of Gen-1 WITR using UKF

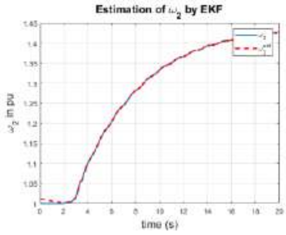


Fig 4.7- Rotor speed of Gen-2 WOTR using EKF

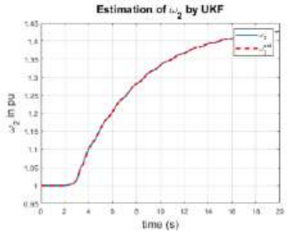


Fig 4.8- Rotor speed of Gen-2 WOTR using UKF

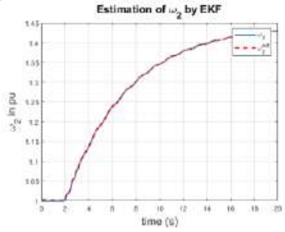


Fig 4.9- Rotor speed of Gen-2 WITR using EKF

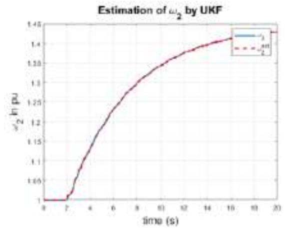


Fig 4.10- Rotor speed of Gen-2 WITR using UKF

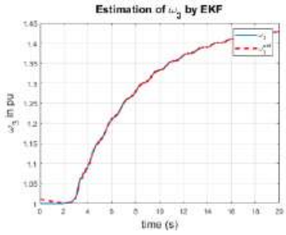


Fig 4.11- Rotor speed of Gen-3 WOTR using EKF

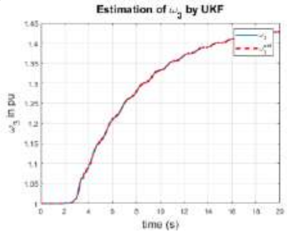


Fig 4.12- Rotor speed of Gen-3 WOTR using UKF

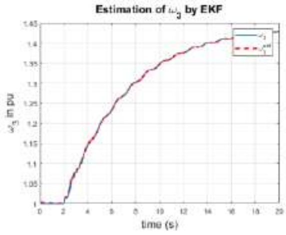


Fig 4.13- Rotor speed of Gen-3 WITR using EKF

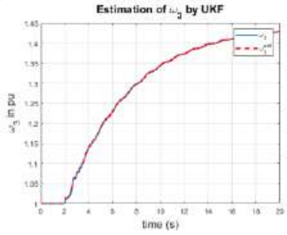


Fig 4.14- Rotor speed of Gen-3 WITR using UKF

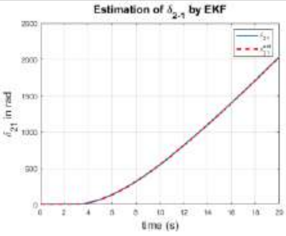


Fig 4.27- Relative Rotor angle of Gen 2-1 WOTR using EKF

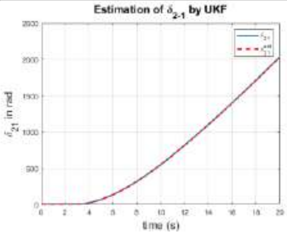


Fig 4.28- Relative Rotor angle of Gen 2-1 WOTR using UKF

Impact Factor 7.047 ⋇ Vol. 10, Issue 4, April 2022

DOI: 10.17148/IJIREEICE.2022.10457

| | |
|---|---|
| 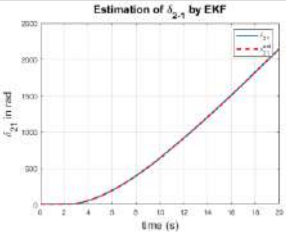 Fig 4.29- Relative Rotor angle of Gen 2-1 WITR using EKF | 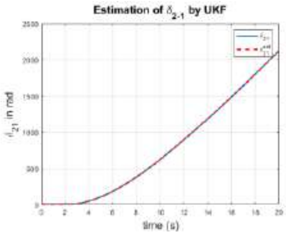 Fig 4.30- Relative Rotor angle of Gen 2-1 WITR using UKF |
| 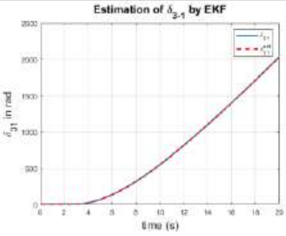 Fig 4.31- Relative Rotor angle of Gen 3-1 WOTR using EKF | 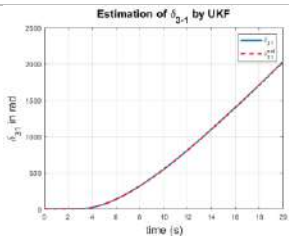 Fig 4.32- Relative Rotor angle of Gen 3-1 WOTR using UKF |
| 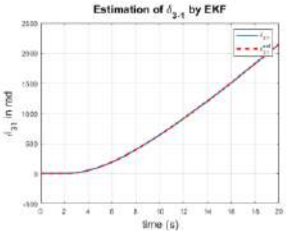 Fig 4.33- Relative Rotor angle of Gen 3-1 WITR using EKF | 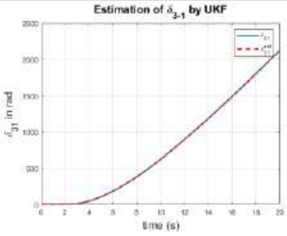 Fig 4.34- Relative Rotor angle of Gen 3-1 WITR using UKF |

**Simulation Results of IEEE-14 bus Using EKF & UKF**

We simulated IEEE-14 bus system when fault near bus 7 is occurs at 2s and stay in system for 0.12s. MATLAB results are presented in next table.

| Without Transient : WOTR \| With Transient : WITR | |
|---|---|
| 5.3.1 Simulation Results using EKF ( WOTR + WITR ) | 5.3.2 Simulation Results using UKF ( WOTR + WITR ) |
| 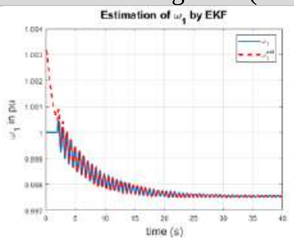 Fig 4.39- Rotor speed of Gen-1 WOTR using EKF | 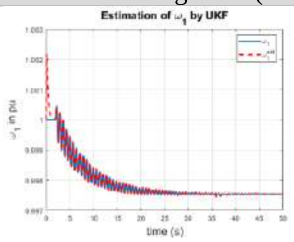 Fig 4.40- Rotor speed of Gen-1 WOTR using UKF |
| 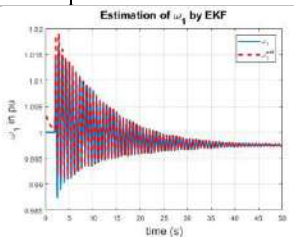 Fig 4.41- Rotor speed of Gen-1 WITR using EKF | 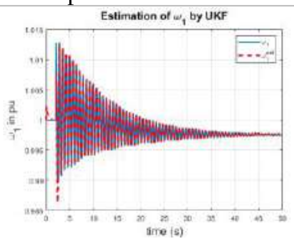 Fig 4.42- Rotor speed of Gen-1 WITR using UKF |

Impact Factor 7.047 ⋇ Vol. 10, Issue 4, April 2022
DOI: 10.17148/IJIREEICE.2022.10457

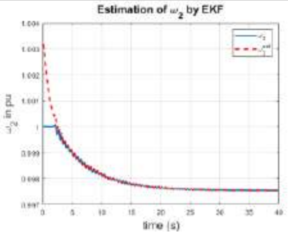


Fig 4.43- Rotor speed of Gen-2 WOTR using EKF

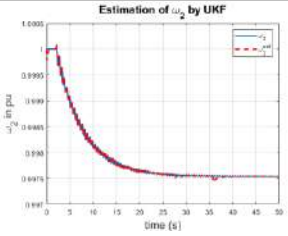


Fig 4.44- Rotor speed of Gen-2 WOTR using UKF

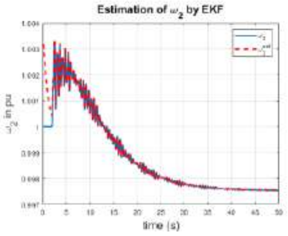


Fig 4.45- Rotor speed of Gen-2 WITR using EKF

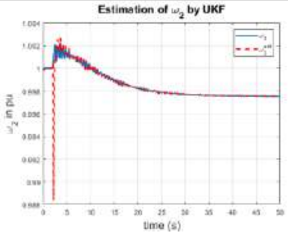


Fig 4.46- Rotor speed of Gen-2 WITR using UKF

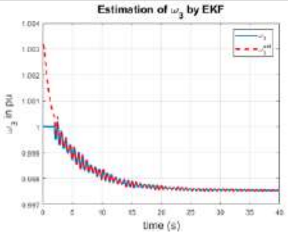


Fig 4.47- Rotor speed of Gen-3 WOTR using EKF

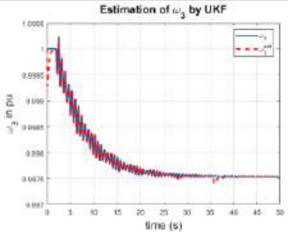


Fig 4.48- Rotor speed of Gen-3 WOTR using UKF

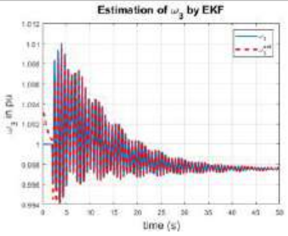


Fig 4.49- Rotor speed of Gen-3 WITR using EKF

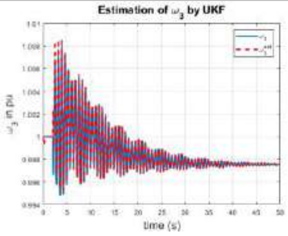


Fig 4.50- Rotor speed of Gen-3 WITR using UKF

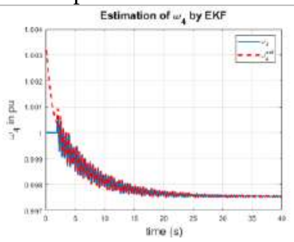


Fig 4.51- Rotor speed of Gen-4 WOTR using EKF

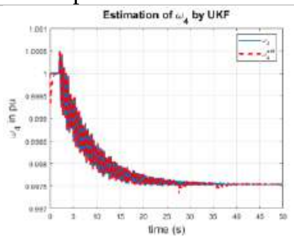


Fig 4.52- Rotor speed of Gen-4 WOTR using UKF

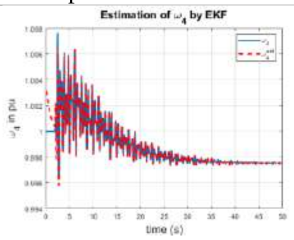


Fig 4.53- Rotor speed of Gen-4 WITR using EKF

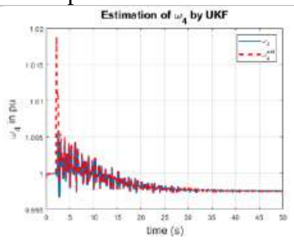


Fig 4.54- Rotor speed of Gen-4 WITR using UKF

DOI: 10.17148/IJIREEICE.2022.10457

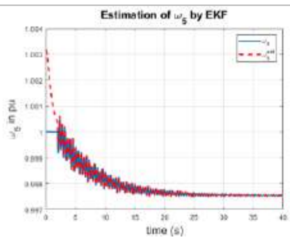

Fig 4.55- Rotor speed of Gen-5 WOTR using EKF

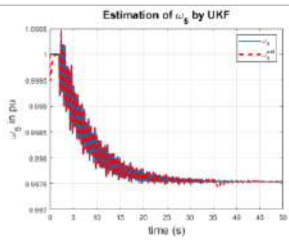

Fig 4.56- Rotor speed of Gen-5 WOTR using UKF

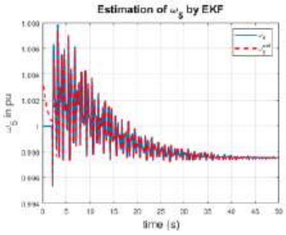

Fig 4.57- Rotor speed of Gen-5 WITR using EKF

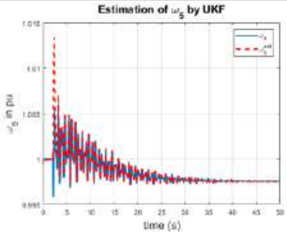

Fig 4.58- Rotor speed of Gen-5 WITR using UKF

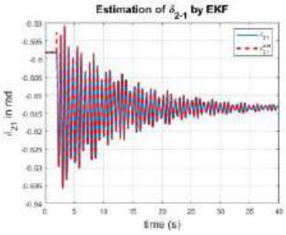

Fig 4.79- Relative Rotor angle of Gen 2-1 WOTR using EKF

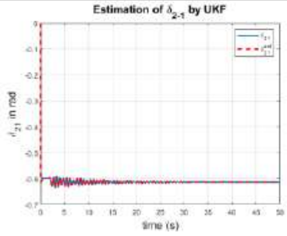

Fig 4.80- Relative Rotor angle of Gen 2-1 WOTR using UKF

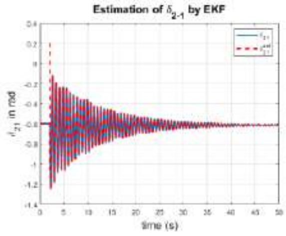

Fig 4.81- Relative Rotor angle of Gen 2-1 WITR using EKF

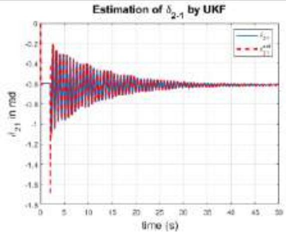

Fig 4.82- Relative Rotor angle of Gen 2-1 WITR using UKF

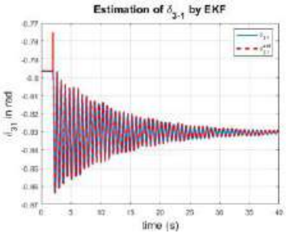

Fig 4.83- Relative Rotor angle of Gen 3-1 WOTR using EKF

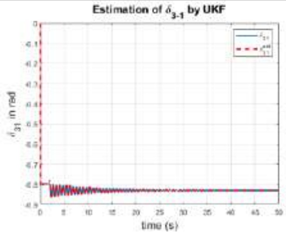

Fig 4.84- Relative Rotor angle of Gen 3-1 WOTR using UKF

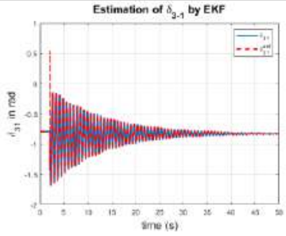

Fig 4.85- Relative Rotor angle of Gen 3-1 WITR using EKF

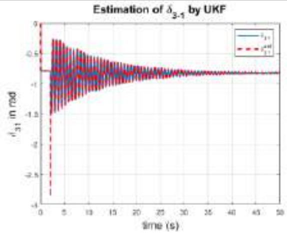

Fig 4.86- Relative Rotor angle of Gen 3-1 WITR using UKF

IJIREEICE ISSN (O) 2321-2004, ISSN (P) 2321-5526

International Journal of Innovative Research in Electrical, Electronics, Instrumentation and Control Engineering

Impact Factor 7.047 ⚟ Vol. 10, Issue 4, April 2022

DOI: 10.17148/IJIREEICE.2022.10457

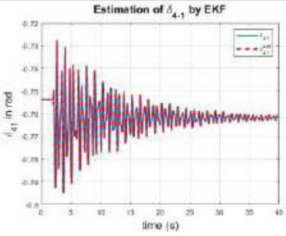


Fig 4.87- Relative Rotor angle of Gen 4-1 WOTR using EKF

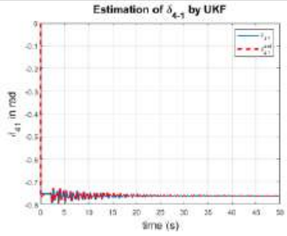


Fig 4.88- Relative Rotor angle of Gen 4-1 WOTR using UKF

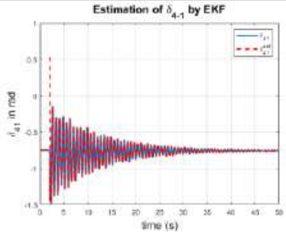


Fig 4.89- Relative Rotor angle of Gen 4-1 WITR using EKF

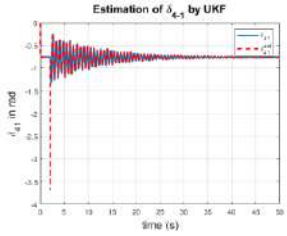


Fig 4.90- Relative Rotor angle of Gen 4-1 WITR using UKF

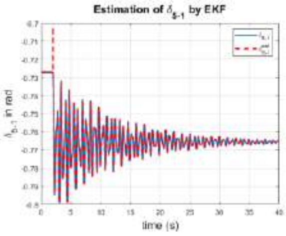


Fig 4.91- Relative Rotor angle of Gen 5-1 WOTR using EKF

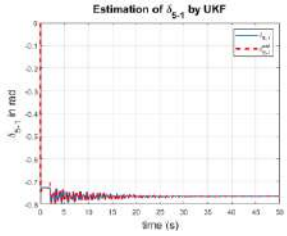


Fig 4.92- Relative Rotor angle of Gen 5-1 WOTR using UKF

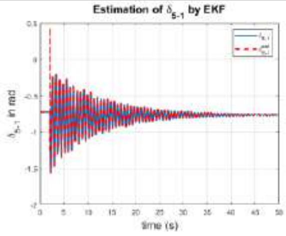


Fig 4.93- Relative Rotor angle of Gen 5-1 WITR using EKF

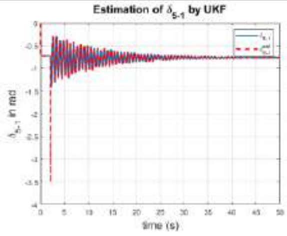


Fig 4.94- Relative Rotor angle of Gen 5-1 WITR using UKF

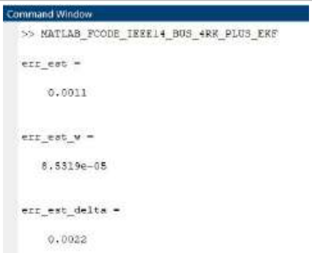

```
Command Window
>> MATLAB_FCODE_IEEE14_BUS_4RK_PLUS_EKF

err_est =

    0.0011

err_est_w =

   8.5319e-05

err_est_delta =

    0.0022
```

Fig 4..95- Estimation Error WOTR using EKF

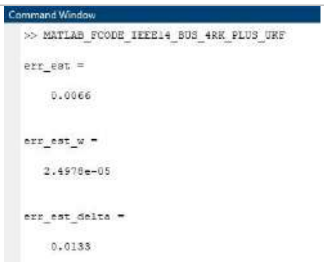

```
Command Window
>> MATLAB_FCODE_IEEE14_BUS_4RK_PLUS_UKF

err_est =

    0.0066

err_est_w =

   2.4978e-05

err_est_delta =

    0.0133
```

Fig 4..96- Estimation Error WOTR using UKF

```
Command Window
>> IEEE14_EKF

err_est =

    0.0013

err_est_w =

   1.0907e-04

err_est_delta =

    0.0024
```

Fig 4..97- Estimation Error WITR using EKF

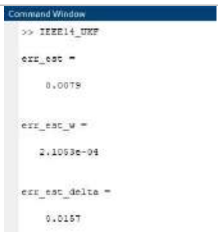

```
Command Window
>> IEEE14_UKF

err_est =

    0.0079

err_est_w =

   2.1053e-04

err_est_delta =

    0.0157
```

Fig 4..98- Estimation Error WOTR using UKF

IJIREEICE ISSN (O) 2321-2004, ISSN (P) 2321-5526

International Journal of Innovative Research in Electrical, Electronics, Instrumentation and Control Engineering

Impact Factor 7.047 ⁜ Vol. 10, Issue 4, April 2022

DOI: 10.17148/IJIREEICE.2022.10457

**Comparison of Simulation result**

| OVERALL ERROR | WSCC-9 BUS | | IEEE-14 BUS | |
|---|---|---|---|---|
| | Without Transient | With Transient | Without Transient | With Transient |
| EKF | 0.011 | 0.066 | 0.0011 | 0.0013 |
| UKF | 0.0623 | 0.0686 | 0.0066 | 0.0079 |

Table 4.1 Overall error using EKF & UKF

| ERROR IN SPEED | WSCC-9 BUS | | IEEE-14 BUS | |
|---|---|---|---|---|
| | Without Transient | With Transient | Without Transient | With Transient |
| EKF | 5.4899e-04 | 3.2457e-04 | 8.5319-e05 | 1.0907e-04 |
| UKF | 1.7567e-04 | 2.7429e-04 | 2.4978-e05 | 2.1053e-04 |

Table 4.2 error in rotor speed estimation using EKF & UKF

| ERROR IN ANGLE | WSCC-9 BUS | | IEEE-14 BUS | |
|---|---|---|---|---|
| | Without Transient | With Transient | Without Transient | With Transient |
| EKF | 0.0016 | 0.0128 | 0.0022 | 0.0024 |
| UKF | 0.1245 | 0.1369 | 0.0133 | 0.0157 |

Table 4.3 error in rotor angle estimation using EKF & UKF

## V. CONCLUSION

During the work in this project, Swing equation is used to determine the speed of rotor and rotor angle with the help of two methods i.e., Extended Kalman Filter (EKF) and Unscented Kalman Filter (UKF). The comparative analysis is also done by using EKF and UKF for WSCC-9 bus system and IEEE-14 bus system through the simulation in MATLAB. Lastly, the transient and steady-state conditions are observed and analyzed for WSCC-9 and IEEE-14 bus system while using EKF and UKF.

Estimation capability and accuracy of Extended kalman filter and unscented kalman filter can be check for more Complex system also considering the transient in the system

Further research can be done on estimated values of generator's rotor speed. Either measured speed of generator can be replace by estimated speed or not. Other dynamic state should be derived by using Extended kalman filter and unscented kalman filter.

## REFERENCES

[1] M. Netto, J. Zhao and L. Mili "A robust extended Kalman filter for power system dynamic state estimation using PMU measurements" 2016 IEEE Power and Energy Society General Meeting (PESGM) (2016).
[2] Farsadi Murtaza, Mohammadzadeh Shahir Farzad and Babaei Ebrahim "Power System States Estimations Using Kalman Filter." 10th International Conference on Electrical & Electronics Engineering (ELECO) (2017).
[3] Montella and Corey "The Kalman Filter and Related Algorithms: A Literature Review" (2011).
[4] Omprakash s. Mankar and Dr. K. Vadirajacharya "Kalman Filter analysis in Dynamic state of power system." Volume: 02 Issue: 06 International Research Journal of Engineering and Technology (IRJET) (Sep-2015).
[5] Bhusal Narayan and Gautam Mukesh "Power System Dynamic State Estimation Using Extended and Unscented Kalman Filters." (2020).
[6] Anupam Saikia and Ram Krishna Mehta "Power system static state estimation using Kalman filter algorithm" int. J. Simul. Multisci. Des. Optim. 2016, 7, A7 (2020).
[7] Dishang D. Trivedi and Santosh C. Vora "performance assessment of EKF and UKF based dynamic state estimators for intermittent measurement data in power system" International Journal of Advanced Research in Engineering and Technology (IJARET) Volume 8, Issue 2, March-April (2017).

International Journal of Innovative Research in Electrical, Electronics, Instrumentation and Control Engineering
Impact Factor 7.047 ⅔ Vol. 10, Issue 4, April 2022
DOI: 10.17148/IJIREEICE.2022.10457

[8] Amouzad Mahdiraji, E., Sedghi Amiri, M., "Improving the Accuracy of the State Estimation Algorithm in the Power System Based on the Location of PMUs and Voltage Angle Relationships". Journal of Engineering Technology and Applied Sciences 5 (3) : 133-147 (2020).
[9] Manoj kumar Rampelli and Debashisha Jena "Advantage of Extended Kalman Filter Over Discrete Kalman Filter In Dynamic State Estimation of Power System Network" IJCTA, 9(10), pp. 4795-4800 (2016).
[10] Hamed Tebianian and Benjamin Jeyasurya "Dynamic state estimation in power systems: Modeling, and challenges" Electric Power Systems Research, Volume 121, Pages 109-114 (2015).